PHYSICAL REVIEW A **78**, 021602(R) (2008)

In situ Ramsey interferometry and diffraction echo with an atomic Fermi gas

C. Marzok, B. Deh, S. Slama, C. Zimmermann, and Ph. W. Courteille
Physikalisches Institut, Eberhard-Karls-Universität Tübingen, Auf der Morgenstelle 14, D-72076 Tübingen, Germany
(Received 20 March 2008; published 12 August 2008)

We report on the observation of Bragg diffraction of a spin-polarized ultracold ^{6}Li Fermi gas and demonstrate a Ramsey-type matter-wave interferometer. Suppression of *s*-wave collisions by the Pauli principle allows for unperturbed dynamics of the atoms in the trap for longer than 2 s. Employing an echo pulse sequence, we observe coherent superpositions of momentum states which do not show any sign of decoherence during the experimentally limited observation time of 100 μs. In contrast, significant decoherence is observed in the presence of a cold cloud of ^{87}Rb atoms. The experiment demonstrates the feasibility of high-resolution atomic interferometry with applications for precision measurements in small volumes and near surfaces.

DOI: 10.1103/PhysRevA.78.021602 PACS number(s): 37.25.+k, 03.75.Ss, 37.10.Jk, 67.85.Pq

Since its first demonstration 30 years ago [1], Bragg diffraction of cold atoms from periodic optical potentials has been established as a standard tool for coherent atom optics. It is successfully used as an interferometric tool both in experiments with atomic beams [2] and Bose-Einstein condensates (BECs) [3] similar to interferometers based on stimulated Raman transitions [4]. A BEC yields high interferometric contrast; however, the lifetime of coherent superpositions is limited due to atomic interaction [5]. Experiments are therefore carried out in diluted clouds during ballistic expansion. Alternatively, adiabatic splitting of the cloud in double-well potentials has been successfully demonstrated recently [6]. Here, interaction-induced number squeezing allows for very long coherence times of 200 ms [7]. By means of Feshbach tuning, the interaction could be tuned to very small values, allowing BECs to perform Bloch oscillations in vertical standing waves for up to 11.5 s [8].

Spin-polarized atomic Fermi gases are interaction-free without the technical demand of Feshbach tuning because the Pauli principle excludes *s*-wave scattering while higher partial waves are suppressed for ultracold temperatures [9]. Hence, phase-sensitive phenomena are expected to exhibit coherence times exceeding those of Bose systems. This has been demonstrated with Bloch oscillations in optical lattices [10], which is so far the only phase-sensitive experiment with fermionic atomic gases. Reference [10] motivated the present work, which now studies a fully tunable fermionic matter-wave interferometer with two spatially separated interferometer arms. Our setup combines the advantages of advanced interferometer schemes for condensates [11] with the expected long coherence times of spin-polarized fermionic clouds. As a result, we can demonstrate the feasibility of fermionic atom interferometry with high phase sensitivity and high spatial resolution. Possible applications range from precision measurements in small volumes [12] to probing fundamental interactions between atoms and surfaces such as Casimir-Polder and van der Waals forces [11].

In the experiment, Bragg interferometry is carried out with ultracold fermionic spin polarized ^{6}Li atoms inside a magnetic trap. We find that after single-pulse diffraction the initial momentum distribution is periodically restored within a time period that corresponds to the trap period. More than 100 of such revivals can be observed within several seconds. This suggests a very long coherence time also for the phases of the atomic wave functions similar to [13]. In contrast, the presence of an additional interacting gas of ^{87}Rb atoms introduces collisions which quickly damp out the revivals. The introduction of a second diffraction pulse delayed by a variable time interval leads to a Ramsey-type interferometer scheme (see, e.g., [14]). Since the different velocity classes within the Fermi gas correspond to different detunings of the interferometer, a complete Ramsey spectrum can be recorded in a single absorption image of the diffracted cloud. Long time intervals between the two Ramsey pulses increase the sensitivity of the interferometer by reducing the fringe spacing. The maximum sensitivity is thus given by the resolution limit of the imaging system. This limitation can be overcome by an echo technique. The deterministic dephasing between atoms in different velocity classes can be inverted by a third diffraction pulse during the Ramsey interval. Such rephasing of coherent superpositions of atomic excitations is well known from spin echo [15] and from experiments with beams of ultracold atoms [4] as well as with trapped clouds [16]. Similarly, for a $\frac{\pi}{2}$-π-$\frac{\pi}{2}$ pulse sequence, we observe an echo-type revival of the diffraction pattern. Such diffraction echo features very robust signatures for the degree of coherence of momentum superposition states. We cannot detect any sign of decoherence within the experimental observation time of 100 μs. For longer times the signal dephases due to the oscillatory motion of the atoms in the trap which mixes the momentum and position of the atoms.

The procedure we use for cooling a mixture of ^{6}Li and ^{87}Rb atoms has been reported in a previous paper [17]. In short, the two species are simultaneously collected by a magneto-optical trap and then transferred via several intermediate magnetic traps into a Ioffe-Pritchard-type trap, where they are stored in their respective hyperfine states $|3/2,3/2\rangle$ and $|2,2\rangle$. Two trap configurations are used in the experiment. The first (compressed) trap is characterized by the secular frequencies $(\omega_x,\omega_y,\omega_z)/2\pi=(762,762,190)$ Hz for ^{6}Li and the magnetic field offset 3.5 G. For ^{87}Rb the trap frequencies are $\sqrt{87/6}$ times lower. The ^{87}Rb cloud is selectively cooled by microwave-induced forced evaporation. The ^{6}Li is sympathetically cooled via interspecies thermalization. For the experiments described below, we typically reach temperatures of a few hundred nanokelvin with

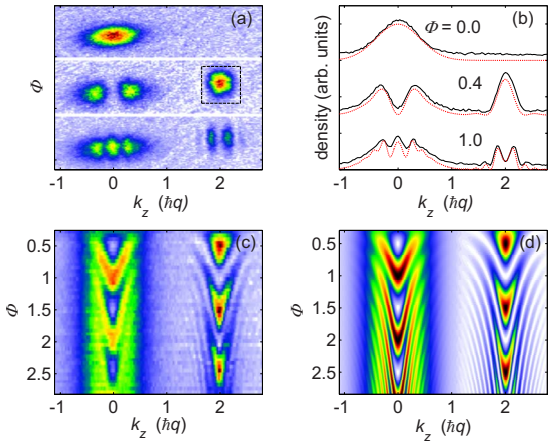

FIG. 1. (Color online) (a) Time-of-flight absorption images of a 1 μK cold cloud after a single Bragg scattering pulse and a 2 ms ballistic expansion period. From top to bottom the Bragg pulse area is varied, $\Phi \equiv \Omega_R \tau/2\pi = 0$, 0.4, and 1. The observed Rabi frequency is $\Omega_R/2\pi = 58$ kHz. (b) The black, solid lines show the integration of the time-of-flight absorption images shown in (a) along the radial direction. The red dotted lines show simulations of the axial momentum distributions with no free parameters. (c) False color map of measured momentum distributions for pulse areas varied from 0 to 6π. The radially integrated absorption images appear as rows. (d) False color map of the calculated momentum distributions using the experimental parameters.

3×10^6 ^{87}Rb atoms and 1.2 μK with 2×10^5 ^{6}Li atoms.

All experiments, unless stated otherwise, are carried out in a second (decompressed) trap characterized by the secular frequencies $(\omega_x, \omega_y, \omega_z)/2\pi = (236, \sim 180, 141)$ Hz for ^{6}Li. In this trap, the different gravitational sagging of the ^{87}Rb and ^{6}Li clouds separates them in space. Consequently, the ^{6}Li cloud does not thermalize and acquires an anisotropic momentum distribution upon decompression. For the z axis we measure a momentum width corresponding to the temperature $T_z \simeq 0.9$ μK.

Bragg diffraction is performed using two laser beams counterpropagating along the z axis and tuned $\Delta_L = 1$ GHz to the red from the low-frequency hyperfine component of the D_2 line of ^{6}Li. Their frequencies differ by $\delta = 2\hbar q^2/m = 2\pi \times 295$ kHz, where $q = 2\pi/\lambda$, $\lambda = 670.977$ nm, and m is the atomic mass. The lasers are phase locked by means of electronic feedback. The Bragg beams have intensities $I_1 = I_2 = 13.7 - 132$ mW/cm^2 corresponding to two-photon Rabi frequencies of $\Omega_R = \Omega_1 \Omega_2 / 2\Delta_L = 2\pi(58 - 450)$ kHz with one-photon Rabi frequencies $\Omega_i = \sqrt{6\pi c^2 \Gamma I_i / \hbar \nu^3}$. Before applying the first Bragg pulse, the ^{87}Rb atoms are removed from the trap with a resonant light pulse. After the Bragg pulse, we wait for half an oscillation period to rephase the momentum distribution before we switch off the trapping field and map the momentum distribution after 2 ms of ballistic expansion by absorption imaging.

The second image of Fig. 1(a) shows a ^{6}Li absorption image taken after a single Bragg pulse whose length τ corresponds to $\Omega_R \tau \approx \pi$. For low Rabi frequencies, only a narrow slice is cut out of the fermionic momentum distribution. The position of the slice along the z axis depends on the

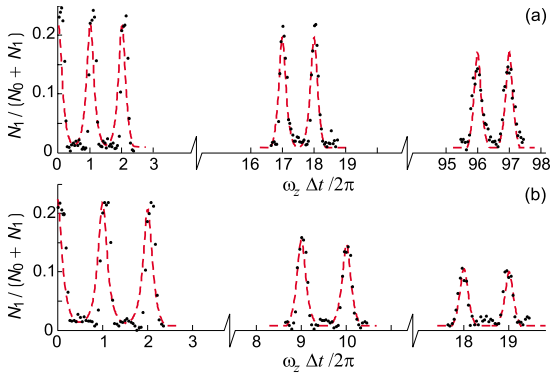

FIG. 2. (Color online) Periodic revival of the momentum distribution in the trap in the absence (a) and in the presence (b) of ^{87}Rb. The population of the state $2\hbar q$ is given relative to the total number of atoms in states $0\hbar q$ and $2\hbar q$, denoted N_0 and N_1, respectively. Neighboring peaks are separated by a full trap period. The dashed line gives an array of Gaussian functions, whose amplitudes are decreasing exponentially in time. The fits to the data yield the decay times of 2.4 s for (a) and 0.15 s for (b). The oscillation frequency is $\omega_z/2\pi = 142.51$ Hz and the Rabi frequency $\Omega_R/2\pi = 58$ kHz.

detuning of the Bragg lasers from the two-photon recoil shift, $\Delta = \delta - 2\hbar q^2/m$; the width is due to power broadening by the Rabi frequency Ω_R. For longer pulses, some of the diffracted atoms scatter back into their initial momentum class and the momentum distribution acquires a more complicated, axially modulated shape. The different momentum classes of the atomic cloud are individually Doppler detuned from the Bragg condition and therefore experience different effective Rabi frequencies.

The experimental data can be well described by a theoretical simulation [Figs. 1(b),1(d)]. In our model we assume that for every atom the Bragg lasers couple only two discrete momentum states. The evolution of every momentum class is calculated individually from the Schrödinger equation. The sum of the results is weighted with the initial momentum distribution. As long as the evolution of the momentum distribution under the action of the trapping potential is not taken into account, the above model applies only to short pulse sequences, $\tau \ll 2\pi/\omega_z$.

To study the impact of both the trap and of collisions on the momentum distribution, we apply a single π pulse, let the atoms oscillate in the trap for a long time $t \gg 2\pi/\omega_z$, and then image the cloud's momentum distribution. This experiment is performed in the compressed trap, which allows spatial overlap between ^{6}Li and ^{87}Rb. By counting the number of atoms in the $2\hbar q$ state as indicated in Fig. 1(a) by the dashed box, we obtain the curves shown in Fig. 2(a) for the case of no ^{87}Rb inside the trap. Clearly, the momentum distribution is restored more than a hundred times with only small damping corresponding to an exponential decay time of 2.4 s. This extremely long dephasing time impressively demonstrates that diffusion in momentum space is very slow [18]. As collisions are forbidden by the Pauli principle, the phase dynamics are fully coherent. The decay of the signal can be associated with dephasing caused by residual anharmonicities of the trapping potential. In this respect the Fermi gas efficiently emulates the dynamics of an ideal gas of non-

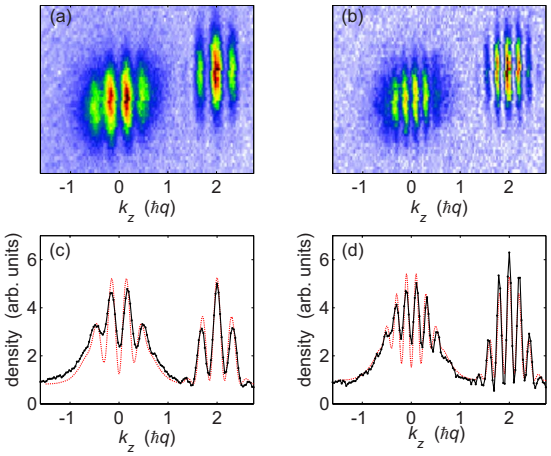

FIG. 3. (Color online) (a),(b) Time-of-flight absorption images taken after a Ramsey pulse sequence and (c),(d) their radial integrations (black solid line). The times between the Ramsey pulse are (a),(c) 6 μs and (b),(d) 12 μs. The theoretical curves (red dotted line) in (b),(d) are fits based on our model. $\omega_z/2\pi=142.51$ Hz and $\Omega_R/2\pi=58$ kHz are as in Fig. 1.

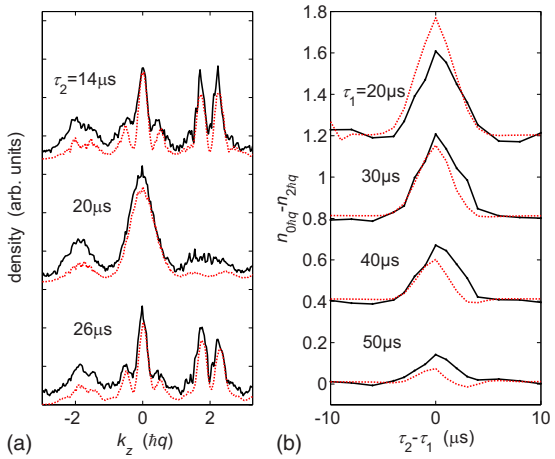

FIG. 4. (Color online) (a) Radially summed absorption images (black solid line) taken after an echo sequence $\pi/2$-τ_1-π-τ_2-$\pi/2$ for $\tau_1=20$ μs. Also shown are simulated momentum distributions calculated with experimental parameters (red dotted line). The calculations include trap motion of atoms with different initial positions weighted with a Boltzmann distribution. Coarse graining of the numerical result due to the limited amount of initial positions included for reasons of finite computing power has been smoothed out by a running average along the momentum axis. (b) Difference of the measured (black solid line) and simulated (red dotted line) relative populations of the states $k_z=0\hbar q$ and $k_z=2\hbar q$ for varying τ_2 with different fixed values of τ_1. The echo signal washes out for τ_1 times larger than 50 μs.

interacting particles. We test the impact of collisions by keeping the ^{87}Rb in the trap. For this case, Fig. 2(b) shows a dramatic reduction of the decay time for the ^{6}Li cloud to 150 ms. This value agrees well with the inverse collision rate estimated for the densities and temperatures specified above, $\gamma_{\mathrm{coll}}^{-1}\simeq 0.11$ s [17,19].

To further study the phase coherence of the momentum state superpositions, we apply a Ramsey pulse sequence of two $\pi/2$ pulses separated by a variable time $\Delta t \ll 2\pi/\omega_z$ similar to [14]. The inhomogeneous initial momentum distribution of the atoms corresponds to a Doppler shift, which detunes the atoms from the resonant Bragg condition. Therefore, the atoms accumulate different phases during their free evolution in the trap, which allows one to observe a full Ramsey spectrum in a single shot (Fig. 3). While we observe Ramsey fringes for $\Delta t \leqslant 32$ μs, for longer times, the fringe spacing is below the resolution limit of the imaging system. Lower temperatures improve the fringe contrast without influencing the fringe spacing. The resolution can also be enhanced by longer times of flight at the expense of contrast.

Longer observation times can be obtained with echo interferometry [4,16]. Here, the free evolution time in a Ramsey experiment is divided into two periods separated by a π pulse. The π pulse inverts the accumulated atomic phase delay of the different momentum classes and the states rephase during the time interval after the π pulse. Thus, all momentum classes can contribute to the signal. The momentum distributions observed after an echo sequence in the regime of *small* Rabi frequencies $\Omega_R \ll \hbar k_{\mathrm{th}}^2/2m$, where k_{th} is the thermal momentum spread, exhibit a central dip for atoms near $2\hbar q$, whose width depends on Ω_R (data not shown). Theoretical simulations show that low-energy atomic momentum classes, which are within the area of this dip, are efficiently rephased by the echo pulse scheme and the $2\hbar q$ state is significantly depopulated by the second $\pi/2$ pulse. In the presence of decoherence, however, the dip vanishes. The appearance of the dip in the momentum profile thus represents a robust signature for coherence, preferable to Ramsey fringes as it overcomes limits in momentum resolution. However, better signal-to-noise ratios are achieved for *higher* Rabi frequencies $\Omega_R \geqslant \hbar k_{\mathrm{th}}^2/2m$. Here, the echo dip encompasses the whole cloud and all atoms in the momentum states around $0\hbar q$ and $2\hbar q$ participate. In Fig. 4, diffraction echo is demonstrated for $\Omega_R/2\pi=220$ kHz. A $\frac{\pi}{2}$-π-$\frac{\pi}{2}$ pulse sequence with delay times of τ_1 and τ_2 between the pulses is applied. In Fig. 4(a) diffraction echo manifests itself in an almost complete revival of the $k_z=0\hbar q$ momentum state when $\tau_1=\tau_2=20$ μs. As is apparent in the data, the $k_z=-2\hbar q$ state is also slightly populated as one approaches the crossover regime from Bragg scattering to Kapitza-Dirac scattering [20]. An extended model including higher-momentum states as well as trap oscillations successfully reproduces the measured momentum distributions (red dotted line). The initial spatial distribution is also taken into account for each k_z individually. Subtracting the population of state $2\hbar q$ from state $0\hbar q$ shows the quantitative effect of diffraction echo [Fig. 4(b)]. The echo signal fades out after $\tau_1+\tau_2=100$ μs. We interpret this effect as deterministic dephasing inside the trap since momentum states are not eigenstates of a harmonic potential. This assumption is supported by our theoretical model, which also predicts a revival after one trap period ($\tau_1=\tau_2=2\pi/\omega_z$) for very low temperatures. A similar trap-induced revival of the interference signal has already been observed for interacting BECs [13], showing the validity of the approach. We looked for such revivals but have so far not observed them. Possible reasons could be an incomplete refocusing of the atomic phases due

to fluctuating Ramsey pulse lengths, power or frequency fluctuations of the Bragg lasers, or alignment imperfections of the Bragg beams with respect to the z axis.

In conclusion, we have demonstrated that atomic Fermi gases are advantageous systems for high-resolution matter-wave interferometry. They are different from Bose gases in that the absence of practically any decoherence mechanism opens up very promising perspectives for applications in fundamental physics as well as for highly sensitive detection of forces in small volumes and near surfaces. Even for trapped atoms, echo techniques produce robust signatures of coherence for interferometric observation times limited to date by imperfections of the experimental setup. No decoherence was observed for times up to 100 μs. The robust coherence of a Fermi gas can also be exploited for Bragg spectroscopy. With this method the dispersion relations and the dynamic structure factors of atomic [21] and molecular condensates [22] have been measured and signatures of vortices [23] were accessible. Similarly to experiments with BECs [21], strong interaction in ^{6}Li-^{87}Rb mixtures could be studied by frequency shifts in Bragg resonances. Interactions can be tuned with the recently found heteronuclear Feshbach resonances [24]. Bragg spectroscopy also allows for mapping the *in situ* momentum distribution of pure ^{6}Li. This direct method of determining the temperature of a trapped gas rivals usual time-of-flight methods, particularly for light ^{6}Li atoms. Details will be reported elsewhere.

This work has been supported by the Deutsche Forschungsgemeinschaft (DFG) within the Schwerpunktprogramm SPP1116. We acknowledge helpful discussions with Andreas Günther and Martin Zwierlein.

[1] P. J. Martin, B. G. Oldaker, A. H. Miklich, and D. E. Pritchard, Phys. Rev. Lett. **60**, 515 (1988).
[2] D. M. Giltner, R. W. McGowan, and S. A. Lee, Phys. Rev. Lett. **75**, 2638 (1995).
[3] Y. Torii *et al.*, Phys. Rev. A **61**, 041602(R) (2000); J. E. Simsarian *et al.*, Phys. Rev. Lett. **85**, 2040 (2000).
[4] M. Kasevich and S. Chu, Phys. Rev. Lett. **67**, 181 (1991).
[5] S. Inouye *et al.*, Science **285**, 571 (1999).
[6] Y. Shin *et al.*, Phys. Rev. Lett. **92**, 050405 (2004); T. Schumm *et al.*, Nat. Phys. **1**, 57 (2005).
[7] G. B. Jo *et al.*, Phys. Rev. Lett. **98**, 030407 (2007).
[8] M. Gustavsson *et al.*, Phys. Rev. Lett. **100**, 080404 (2008); M. Fattori *et al.*, *ibid.* **100**, 080405 (2008).
[9] B. DeMarco, S. B. Papp, and D. S. Jin, Phys. Rev. Lett. **86**, 5409 (2001).
[10] G. Roati, E. de Mirandes, F. Ferlaino, H. Ott, G. Modugno, and M. Inguscio, Phys. Rev. Lett. **92**, 230402 (2004).
[11] O. Garcia, B. Deissler, K. J. Hughes, J. M. Reeves, and C. A. Sackett, Phys. Rev. A **74**, 031601(R) (2006).
[12] S. Dimopoulos and A. A. Geraci, Phys. Rev. D **68**, 124021 (2003).
[13] M. Horikoshi and K. Nakagawa, Phys. Rev. Lett. **99**, 180401 (2007).
[14] K. Bongs *et al.*, Phys. Rev. A **63**, 031602(R) (2001).
[15] E. L. Hahn, Phys. Rev. **80**, 580 (1950).
[16] F. B. J. Buchkremer, R. Dumke, H. Levsen, G. Birkl, and W. Ertmer, Phys. Rev. Lett. **85**, 3121 (2000); M. F. Andersen, A. Kaplan, and N. Davidson, *ibid.* **90**, 023001 (2003); E. Gershnabel *et al.*, Phys. Rev. A **69**, 041604(R) (2004).
[17] C. Silber *et al.*, Phys. Rev. Lett. **95**, 170408 (2005).
[18] In the decompressed trap, $\omega_z/2\pi=140.89$ Hz, we found dephasing times without ^{87}Rb atoms exceeding 13 s.
[19] C. Marzok, B. Deh, Ph. W. Courteille, and C. Zimmermann, Phys. Rev. A **76**, 052704 (2007).
[20] P. L. Gould, G. A. Ruff, and D. E. Pritchard, Phys. Rev. Lett. **56**, 827 (1986).
[21] J. Stenger *et al.*, Phys. Rev. Lett. **82**, 4569 (1999); J. Stenger *et al.*, Appl. Phys. B: Lasers Opt. **69**, 347 (1999); D. M. Stamper-Kurn *et al.*, Phys. Rev. Lett. **83**, 2876 (1999); D. M. Stamper-Kurn and W. Ketterle, in *Coherent Atomic Matter Waves*, edited by R. Kaiser, C. Westbrook, and F. David, Proceedings of the Les Houches Summer School of Theoretical Physics, Course LXXII, 1999 (Springer, New York, 2001); J. Steinhauer, R. Ozeri, N. Katz, and N. Davidson, Phys. Rev. Lett. **88**, 120407 (2002).
[22] J. R. Abo-Shaeer *et al.*, Phys. Rev. Lett. **94**, 040405 (2005).
[23] P. B. Blakie and R. J. Ballagh, J. Phys. B **33**, 3961 (2000); Phys. Rev. Lett. **86**, 3930 (2001); S. R. Muniz, D. S. Naik, and C. Raman, Phys. Rev. A **73**, 041605(R) (2006).
[24] B. Deh, C. Marzok, C. Zimmermann, and Ph. W. Courteille, Phys. Rev. A **77**, 010701(R) (2008).